Fuel 158 (2015) 388–398

Contents lists available at ScienceDirect

Fuel

journal homepage: www.elsevier.com/locate/fuel

Evaluation of heat sink capability and deposition propensity of supercritical endothermic fuels in a minichannel

Zhaohui Liu [a], Qincheng Bi [a,*], Jiangtao Feng [b]

[a] State Key Laboratory of Multiphase Flow in Power Engineering, Xi'an Jiaotong University, Xi'an 710049, PR China
[b] Department of Environment Science and Technology, School of Energy and Power Engineering, Xi'an Jiaotong University, Xi'an 710049, PR China

HIGHLIGHTS

- A set of approaches were proposed for heat sink and deposition propensity evaluation.
- Cyclohexane, n-hexane and toluene and two endothermic fuels were investigated.
- Volumetric heat sink and anti-coking capability were two contrary features.
- Cyclohexane had high heat sink and good anti-coking characteristics.
- Coking propensity ranked as: endothermic fuel > cyclohexane > n-hexane > toluene.

ARTICLE INFO

Article history:
Received 8 February 2015
Received in revised form 23 May 2015
Accepted 29 May 2015
Available online 3 June 2015

Keywords:
Endothermic fuel
Hydrocarbons
Coking
Heat sink
Pyrolysis

ABSTRACT

The aim of this study was to develop approaches for the evaluation of heat sink capabilities and deposition propensities of different endothermic fuels in a minichannel. It should be noted that compared with our previous paper [23] which proposed the hydraulic resistance method (HRM) and validated it using one fuel pyrolyzed at different fluid temperatures, the significant one of the innovative points of this paper is that the HRM was corrected and applied to evaluate five different hydrocarbons, which are three pure hydrocarbons (cyclohexane, n-hexane and toluene), one petroleum-derived fuel and one synthetic fuel that were modeled as endothermic fuels. All of these fuels were tested in a minichannel with an internal diameter of 2.0 mm. The qualities of high volumetric heat sink capacity and good anti-coking capability were proven to be two contrary features in endothermic fuels. All of the five hydrocarbons tested had a mass heat sink of approximately 3.4 MJ/kg at a temperature of 750 °C and pressure of 5 MPa. However, the volumetric heat sinks (per unit volume hydrocarbon at the standard condition) were considerably different due to the hydrocarbons' varying densities. Overall, cyclohexane showed better performance than the other four hydrocarbons, as it had a relatively high volumetric heat sink and good anti-coking characteristics. The coking runs were designed for a steady state at a bulk fluid temperature of 750 °C for 20 min, which allowed measureable coke deposition layers to accumulate on the channel's inside surface. Another innovative point is that except the HRM, methods used to assess the deposition propensity included pressure drop changes during the coking run process, measurements of coke deposition in the filter, observations of the color features of liquid products and the weighing method, all of those methods are aided for the HRM to better differentiate the deposition propensity for different fuels. These different methods yielded a common conclusion that the coke deposit rates of the tested hydrocarbons could be ranked as follows: endothermic fuel > cyclohexane > n-hexane > toluene. It was found, however, that the deposit thickness was only one of the factors affecting heat transfer performance for different hydrocarbons, and the thickness was far from sufficient to reduce the heat transfer that led to the increased wall temperatures.

1. Introduction

Endothermic fuels [1–3] have been used as coolants in regeneratively cooled hypersonic vehicles, as they help to remove the

Abbreviations: HRM, hydraulic resistance method; TC, thermocouples; CBO, carbon burn-off method; WEDM, wire electrical discharge machining; PAH, polycyclic aromatic hydrocarbons.

* Corresponding author. Tel.: +86 (0)29 82665287.
E-mail address: qcbi@mail.xjtu.edu.cn (Q. Bi).

http://dx.doi.org/10.1016/j.fuel.2015.05.068
0016-2361/

enormous excessive heat from engine structures exposed to supersonic combustion. These fuels should persist for relatively long periods at high temperatures and cause no significant coke deposition [4]. The operations of air-breathing hypersonic vehicles are definitely different from those of rockets, as these vehicles undergo huge heat fluxes and must operate with limited quantities of coolant fuel. The wide temperature range generates strong chemical reactions in the cooling structures. In general, the convective cooling of endothermic fuel in the cooling structure involves a complex process of fluid flow and heat transfer, with chemical reactions occurring in minichannels under supercritical conditions.

The efficiency and performance of fuels have been greatly improved in the last 100 years [4]. The concept of "Endothermic fuel" was first proposed in 1971 [1], and it will provide significant new capabilities in the future. It is a big challenge to find an endothermic fuel that can improve heat sink capability with limited coking to deal with the high heat flux and surface temperature in the supersonic combustion chamber. Many investigations of endothermic fuel have been conducted since 1990, including studies on heat sink measurement [5,6], heat transfer and coking behavior [7,8], the factors that influence pyrolysis and coking [4,9–15], fluid flow instability and heat transfer [16], the hydraulic effect and thermal effect caused by coking [17] and the thermal physical properties of fuels [18–21].

In recent decades, one of the most popular methods for measuring coke deposition on a channel's inner surface was the carbon burn-off (CBO) method [9,22]. In this method, the reaction channel was cut into sections, then washed in n-heptane to remove residual fuel and dried in a vacuum oven at 100 °C for a minimum of 12 h. As a last step, a LECO RC-412 Multiphase Carbon Determinator was used to oxidize the carbon and complete the coke measurement for each section. However, this CBO was an off-line method that required tedious work to cut the test channel into sections. The hydraulic resistance method (HRM) we propose [23] is an on-line method that can be easily implemented to measure the equivalent coke deposition amount in a minichannel. This method involves a process based on Poiseuille flow for measuring the change in hydraulic resistance following the reaction.

This study used the HRM and compared its results with those of several other approaches for conveniently evaluating the heat sink capabilities and deposition propensities of supercritical endothermic fuels in a minichannel. Noted that compared with our previous paper [23] which proposed the HRM and validated it using one fuel pyrolyzed at different fluid temperatures, in this paper the HRM was corrected and applied to evaluate five different hydrocarbons, which are three pure hydrocarbons (cyclohexane, n-hexane and toluene), one petroleum-derived fuel and one synthetic fuel that were modeled as endothermic fuels. And except the HRM, methods used to assess the deposition propensity included pressure drop changes during the coking run process, measurements of coke deposition in the filter, observations of the color features of liquid products and the weighing method, all of those methods are aided for the HRM to better differentiate the deposition propensity for different fuels. The results documented in this study can be used to select excellent fuel candidates with desired heat sink and coking properties. This study can also serve as a guide for the design of endothermic fuels.

2. Experimental setup and materials

An electrically heated channel (made of nickel alloy steel GH3128 [6] from China) was used to simulate the cooling passage of an engine structure exposed to supersonic combustion. GH3128 tubing was selected for its tolerance in working temperatures up to 1000 °C. The catalytic activity of nickel could affect the growth, shape and formation of coke deposition [2], but the main focus of this experiment was to evaluate the amounts of coke deposited by each kind of fuel (rather than to examine the thermal cracking and coke formation mechanism). The experimental system has been described in detail in our previous reports [24–26].

Fig. 1 shows the test sections, which included two channels, both with inside diameter of 2.0 mm. The diabatic channel (total length: 800 mm; heated length: 720 mm), which was heated by low voltage alternating electrical current, was the main test section designed for the evaluation of the heat sink and coking characteristics. The unheated adiabatic channel (length: 200 mm) was set up to aid with characterization of the deposition propensity, although this channel does not really exist in a practical scramjet. The reacted fuel at high temperature passed through a filter at the end of the adiabatic channel and then exited the test facility. Both of the test channels were wrapped in thermal insulation cotton on the outside to reduce heat loss.

The hydrocarbons were fed into the channels by a dosing pump (Elite P500, from China) with a constant mass flow rate (flow stability: ±0.5%). A Coriolis mass flow meter at the inlet of the diabatic channel was used to measure the mass flow rate. The outlet pressure and the pressure drop across the test section were measured by Rosemont 3051 transducers. The fluid inlet and outlet temperatures of the test channel were measured by type K sheathed thermocouples with outside diameters of 1.0 mm, which were submerged in the working fluid. Some 15 thermocouples (TCs) of type K, with outside diameters of 0.2 mm, were spot-welded onto the bottom surface of the diabatic channel at intervals of 50 mm for measuring the outside wall temperatures. All of the measured data were input to the computer by an Isolated Measurement Pods 3595 (IMP3595) data acquisition system with a frequency of 1 Hz.

Conventional jet engines can use a broad class of distillate hydrocarbon fuels known as kerosenes, which have carbon number distributions from about C_7 to C_{18} and an average molecular weight of about 150 g/mol [20]. Petroleum-derived fuels consist of a blend of hundreds of hydrocarbons, which can be separated into paraffins, cycloparaffins and aromatics [21]. In this study, five hydrocarbons were selected and evaluated. EHF1 and EHF2 are labeled as two endothermic fuels. EHF1 was a kind of kerosene distilled from

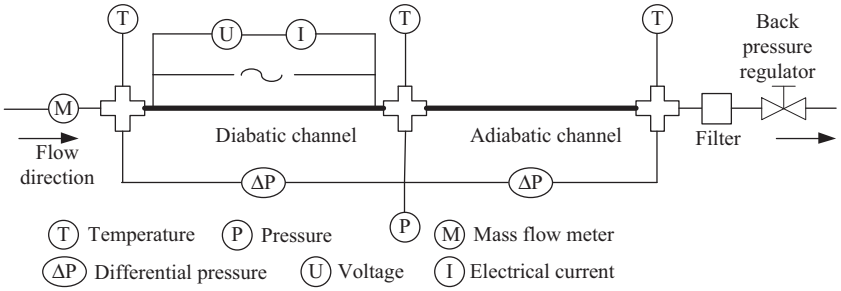

Fig. 1. Schematic diagram of the test sections.

Table 1
Components of the endothermic fuels EHF1 and EHF2.

Components	EHF1	EHF2
Cycloalkanes	82.15 wt.%	63.77 wt.%
Alkanes	10.19 wt.%	0.68 wt.%
Olefins	7.46 wt.%	21.95 wt.%
Aromatics	0	0
Others	0.20 wt.%	13.6 wt.%

petroleum. EHF2 was a synthetic fuel. Table 1 shows their main components. EHF1 and EHF2 are mainly made up of cycloparaffins, but EHF2 also contained considerable olefins such as cyclohexene. EHF1, from Karamay Oilfield in China, has an average molecular formula of $C_{11.9}H_{23.4}$ and a molecular weight of 166.2 g/mol. EHF2 has a formula of $C_{10.6}H_{19.8}$ and a molecular weight of 147.0 g/mol. These two kerosenes have critical pressure of about 2.5 MPa, and critical temperature of about 400 °C. It should be noted that the EHF1 and EHF2 are modeled as but not the really used endothermic fuel in the regeneratively cooled vehicles. Another three pure hydrocarbons (cyclohexane, n-hexane, and toluene) with similar carbon numbers were selected to represent the paraffins, cycloparaffins and aromatics. The critical parameters for the three pure hydrocarbons are (4.1, 3.0, 4.1) MPa and (280.5, 234.7, 318.6) °C respectively. The purities of the cyclohexane, n-hexane and toluene used in the experiment were greater than 99.5%, as stated by the manufacturer (Tianjin Fuchen Chemical Reagent, China).

3. Experimental methods and procedures

3.1. Heat sink measurement

The heat sink (defined as the fluid enthalpy relative to 25 °C) was measured by the energy conservation method. In discerning the thermal balance of heating power Q_h (W) and heat loss to the environment, the mass heat sink Q_m (kJ/kg) can be determined by equation (1).

$$Q_m = Q_h \eta / M \tag{1}$$

where M (g/s) is the mass flow rate, and η is the heat efficiency, which was measured by the heat balance method as a function of the channel's outside surface temperature. The heat efficiency was measured as $\eta < 5.0\%$ for all operating conditions, including fuel temperatures up to 750 °C. The considerable heat efficiency contributed to high fuel temperatures (which led to high wall temperatures up to 900 °C), a relatively low mass flow rate and a large surface to volume ratio for the minichannel. The heat efficiency was experimentally measured by heating the diabatic channel (shown in Fig. 1) without fuel employed. In that case, the heating power was indicated as equal to the heat loss at the corresponding constant wall temperature at a steady state. The results of the heat efficiency test were calibrated and validated by using the adiabatic channel at fuel temperatures from 25 °C to 750 °C. The heating power imposed on the adiabatic channel was indicated as its heat loss while the inlet and outlet fuel temperatures were kept accordant. For example, the heating power of the diabatic channel was 4.7 kW for cyclohexane at fuel outlet temperature of 700 °C and mass flow rate of 1.5 g/s, and the heat loss (the heating power of the following adiabatic channel) was about 230 W (a little less than 5.0%).

3.2. Deposition measurement

The hydraulic resistance method (HRM) described in our previous work [23] is one of the main methods for evaluating coke deposition. In this study, the coking rate was equivalently measured as the average thickness of the coke layer in the test channel. The HRM is based on the principle that as coke deposition constricts the flow area, the flow resistance increases significantly in the minichannel. According to Poiseuille's law, the pressure drop ΔP in the test channel is inversely proportional to the fourth power of the channel's internal diameter D at a given mass flow rate and a constant fluid thermal condition (constant density and viscosity), as shown in equation (2).

$$\Delta P = \frac{128LM\mu}{\rho\pi D^4} = \frac{\text{Constant}}{D^4}M \tag{2}$$

where L is the length of the test channel, and ρ and μ are the density and the viscosity of the fluid flowing through the test channel. Poiseuille's law can be applied at the relative surface roughness inside the channel of $0 < \Delta/D < 0.05$, as has been verified in our previous report [23]. The roughness of the coke layer surface was validated as being much less than 100 μm, which satisfied the assumption for applying Poiseuille's law in the 2.0 mm ID minichannel. The pressure drop change in the test channel due to coke deposition could therefore be used to calculate the equivalent coke thicknesses. As indicated in equation (3), the ratio of the channel diameter after deposition D_2 to that before deposition D_1 could be derived by the slope change of ΔP vs. M at different mass flow rates.

$$\frac{D_2}{D_1} = \sqrt[4]{\frac{\text{slope}_1(\Delta P \text{vs.} M)}{\text{slope}_2(\Delta P \text{vs.} M)}} \tag{3}$$

It should be noted that the coke deposits along the length of the channel were not homogenous, and the uneven depths affected the results of the HRM significantly. In order to involve the effect of the coke deposit profile on the hydraulic resistance of the test channel, in this paper a corrected HRM are suggested to apply in the diabatic channel.

One of the assumptions of the HRM is that coke deposits along the length of the test channel are uniformity. According to the experimental results we found that the deposits along the length of the adiabatic channel are nearly uniformity. Therefore the diameter difference along the adiabatic channel contributed by deposits can be neglected, and the HRM was directly used in the adiabatic channel. But in the diabatic channel the deposit thickness varied from 0 to 150 μm. In order to understand how the deposit profile affects the hydraulic resistance, two corrected models of the coke deposit profiles are constructed and shown in Fig. 2. In the corrected model (a) the deposit thickness h (μm) at the location x (mm) ($h = x{\cdot}H/L$) linearly increases along the length of the whole channel L (mm), the deposit thickness at the entrance is 0 and at the exit is H (μm). Considering the fact that coke produces while fuel pyrolyzes at high temperature, therefore the corrected model (b) assumes that there are no deposit at the front 1/3 length of the

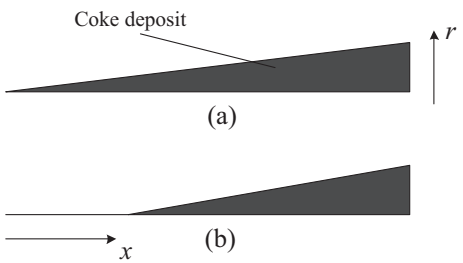

Fig. 2. Two models of coke deposit profiles along the test channel: (a) deposit thickness linearly increases along the whole channel (b) deposit thickness linearly increases along the latter 2/3 length of the channel with no deposit in the front 1/3 length of the channel.

test channel, and at the latter 2/3 length the deposit linearly increases to thickness of H from 0.

In the HRM, the deposit profile cannot be reflected in the diameter calculation by equation (3). In the corrected model (a), the ratio r_a of pressure drop after coking to that before coking was calculated by equation (4). Effects of different average deposit thicknesses on the hydraulic resistance in the minichannel with an internal diameter of 2.0 mm are listed in the Table 2. The average deposit thickness can be also predicted by HRM using the pressure drop ratio r_a. The deviations of the deposit results calculated by HRM with the arithmetic average real values enlarge quickly to 6.8% as an increase in the exit deposit thickness to 150 μm. For model (b), effects of different deposit thicknesses are listed in Table 3. The pressure drop ratios r_b were calculated by equation (5), which were derived from the equation (4) considering no deposit in the front 1/3 length of the test channel. The deviations are much larger than that in model (a). And as the deposit increased to 150 μm at the exit, the deviation of the calculated result from HRM enlarges to 13.8%.

$$r_a = \frac{\overline{\Delta P_2}}{\Delta P_1} = \int \frac{\Delta P_2}{\Delta P_1} dx/L = \left[\int_0^L 1/\left(1-\frac{H}{L}x\right)^4 dx\right]/L = \frac{1}{3H}\left[\frac{1}{(1-H)^3}-1\right] \quad (4)$$

$$r_b = \frac{\overline{\Delta P_2}}{\Delta P_1} = \frac{2}{9H}\left[\frac{1}{(1-H)^3}-1\right]+\frac{1}{3} \quad (5)$$

It indicated that the deposit profile along the test channel had a significant influence on the hydraulic resistance. Therefore in this paper the corrected HRM which using the practical model (b) are suggested. The coke thickness at the exit of the test channel can be predicted by equation (5) using the measured pressure drop ratio or the measured slope ratio shown in Eq. (3). Then the average deposit thickness of the test channel can be evaluated using the deposit profile in the model (b). Noted that in this paper the hydrocarbons were pyrolyzed at the channel outlet fluid temperature of 750 °C, and the hydrocarbons entered the test channel with ambient temperature. Therefore in model (b) in the entrance part of 1/3 length of the channel with fluid temperature less than 400 °C it was considered to have no deposit according to the practical deposit profiles. When the corrected HRM will be applied to other operating conditions, the entrance length with no deposit should be reconsidered to make the model more applicable.

Another condition that should be mentioned is that only when the coking run was completed successfully without the channel being burned out during fuel pyrolysis could the HRM be applied. Certain other methods were also used to aid in representing the coke deposition. These methods involved analyzing the process characteristics of the coking runs, measuring coke depositions in the filter, and assessing the fuel color features after pyrolysis. These methods are described and discussed in the following sections.

Table 2
Effects of the deposit thickness on the hydraulic resistance in the model (a).

H[a] (mm)	$\overline{h}$[b] (mm)	r_a[c]	$\overline{h}_p$[d] (mm)	Deviations[e] (%)
0.050	0.025	1.109	0.026	0.7
0.100	0.050	1.239	0.052	2.9
0.150	0.075	1.396	0.080	6.8

[a] Deposit thickness at the exit of the test channel, the given value in model (a).
[b] Arithmetic average deposit thickness of the test channel: $\overline{h} = H/2$.
[c] Pressure drop ratio calculated by equation (4).
[d] Average deposit thickness predicted by HRM using the pressure drop ratio r_a.
[e] Calculated by the following equation: $\left(\overline{h}_p - \overline{h}\right)/\overline{h} \cdot 100\%$.

Table 3
Effects of the deposit thickness on the hydraulic resistance in the model (b).

H (mm)	$\overline{h}$[a] (mm)	r_b[b]	$\overline{h}_p$ (mm)	Deviations (%)
0.050	0.017	1.073	0.018	4.8
0.100	0.033	1.159	0.036	9.0
0.150	0.050	1.264	0.057	13.8

[a] Arithmetic average deposit thickness of the test channel: $\overline{h} = H/3$.
[b] Pressure drop ratio calculated by equation (5).

3.3. Test procedures for measuring heat sink and deposition propensity

The aim of this study was to develop a set of methods and procedures for determining the heat sink capabilities and deposition propensities of various fuels. The R&D of endothermic fuels is a complicated and ongoing task. Before a new type of fuel can be approved, considerable time and effort is required to test numerous fuel recipes. Therefore, it is important and necessary to simplify and standardize the following test procedures.

3.3.1. Hydraulic resistance measurement before and after a coking run

Each test should be performed on new test channels. Therefore, before and after each coking run at ambient temperature and atmosphere pressure, the pressure drops of the diabatic and adiabatic channels were tested at given mass flow rates at laminar flow condition. The equivalent thickness of deposition could be derived from the pressure drop change before and after coke deposition in accordance with Poiseuille's law, which states that the pressure drop along the channel is inversely proportional to the fourth power of the channel's inside diameter at a given mass flow rate at laminar flow, as shown in Eq. (2).

3.3.2. Heat sink measurement

At a given pressure of 5 MPa and a mass flow rate of 1 g/s, the heat sink was measured at the fluid outlet temperature of the diabatic channel over a range of 50–750 °C at intervals of 50 °C. It took about 90 s to achieve a stable condition after increasing the heat to reach the requested fluid temperature. At each operating condition, the heat sink was measured at steady state. The total time needed for the heat sink measurement did not exceed 40 min. The time required for measuring the heat sink of the hydrocarbons at temperatures above 600 °C did not exceed 5 min. Therefore the coke deposition at temperatures below 750 °C did not have a significant influence on the following coking run.

3.3.3. Coking run

During the coking run, the operation condition was fixed at a steady state, with a fluid outlet temperature of 750 °C for the diabatic channel. This state was maintained as long as possible, up to 20 min, to produce a measureable deposition. If the pressure suddenly rose due to the channel being jammed by coke formation, the coking run would break down. The pressure drops and pressure trends over time were recorded. After the coking runs, the amounts of coke deposits were measured by HRM and the other methods.

These proposed methods and procedures were repeatedly verified to be effective and convenient for evaluating the heat sink capability and deposition propensity of endothermic fuels, as the results obtained for the five hydrocarbons tested in this study demonstrate. The heat sink measurement and coking run could be finished in an hour with a fuel expenditure of about 5 L. The accuracy of the results adequately satisfied the requirements of endothermic fuel evaluation.

3.4. Uncertainty analysis

The standard uncertainties of the mass heat sink and the average coke thickness derived by the corrected HRM were estimated. The standard uncertainties of the TCs were ±0.2 °C at a temperature of $T < 200$ °C, ±0.5 °C at 200 °C $\leqslant T <$ 500 °C, and ±1.0 °C at 500 °C $\leqslant T <$ 800 °C.

The standard relative uncertainty $u_r(Q_m)$ of the mass heat sink Q_m was determined by differentiation of equation (1). Including also the uncertainties of temperature, the combined standard relative uncertainty of Q_m is given in equation (6), where $u_r(X)$ is the standard relative uncertainty and $u(X)$ the standard uncertainty of variable X. The standard relative uncertainty of the heating power Q_h was 1.4%; that of the heating efficiency η was 1.4%; and that of the mass flow rate M was 0.5%. In order to evaluate the effects of the temperature uncertainties, the derivatives $(\partial Q_m/\partial T)$ in equation (6) were estimated from the heat sink results in Fig. 3. It was found that the effects of the temperature uncertainties contributed less than 0.5% to $u_r(Q_m)$. The overall standard relative uncertainties $u_r(Q_m)$ were determined as 2.1%.

$$u_r^2(Q_m) = u_r^2(Q_h) + u_r^2(\eta) + u_r^2(M) + \left[Q_m^{-1}(\partial Q_m/\partial T)u(T)\right]^2 \quad (6)$$

The standard relative uncertainty $u_r(D_2)$ of the internal diameter after deposition D_2 in HRM was determined by differentiation of equation (3). The combined standard relative uncertainty of D_2 is given in equation (7). The standard relative uncertainty of D_1 was 2.1%, and that of the slope S_1 and S_2 was less than 5.0%. Therefore the overall standard relative uncertainty $u_r(D_2)$ was determined as 2.7%, and the average deposit thickness $\bar{h} = (D_1 - D_2)/2$ was estimated as $\sqrt{u_r^2(D_2) + u_r^2(D_1)} = 3.5\%$. The average deposit thickness determined by the corrected HRM was considered to have the same uncertainty of 3.5% as that in HRM, for the equation (4) and (5) for the corrected HRM were developed from the equation (3) for the HRM.

$$u_r^2(D_2) = u_r^2(D_1) + \frac{1}{16}\left[u_r^2(S_1) + u_r^2(S_2)\right] \quad (7)$$

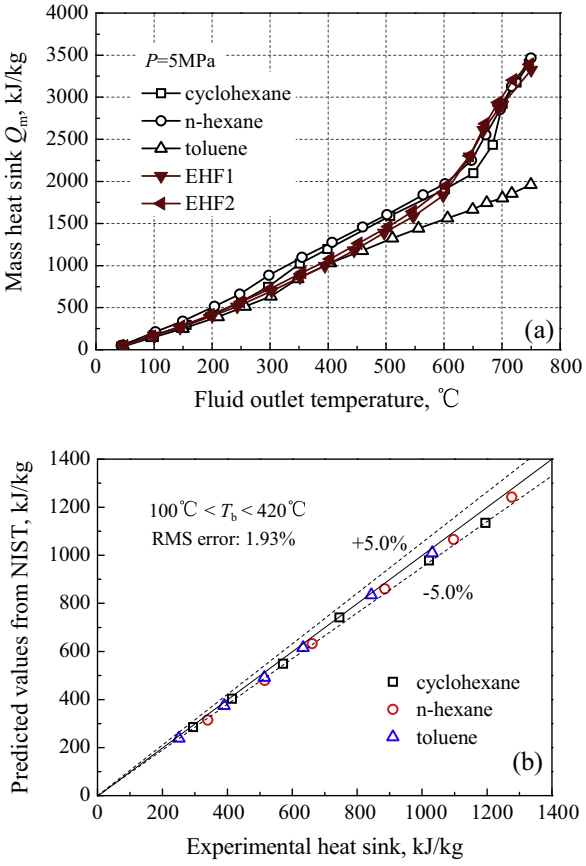

Fig. 3. Results of heat sink tests for the five hydrocarbons.

4. Results of heat sink and deposition propensity

Endothermic fuel can be a complex mixture of cycloalkanes, alkanes and aromatics [21]. For this study, cyclohexane, n-hexane and toluene were selected as classical substances whose heat sink and coke depositions during pyrolysis were tested and compared with the petroleum-derived and synthetic endothermic fuel, labeled as EHF1 and EHF2. The endothermic degradation of the fuel acted as a heat sink. In parallel, the thermal decomposition produced heavy aromatic compounds which could lead to the formation of coke deposits on the reactor surface [15].

4.1. Results of heat sink capability

The term *heat sink* (or cooling capacity) is equivalent in meaning to *enthalpy*. The heat sink of an endothermic fuel consists of the physical heat sink, which arises due to the temperature increase (the sensible heating $C_p\Delta T$), and the chemical heat sink, in which the heat absorption is caused by endothermic reactions. In this study, the mass heat sink related to 25 °C Q_m of the three pure hydrocarbons and the two endothermic fuels at a pressure of 5 MPa were measured as shown in Fig. 3. The heat sink results of the three pure hydrocarbons at 100 °C < T < 420 °C were compared with the predicated values by NIST REFPROP to verify the accuracy of heat sink measurements. Good agreements were obtained between the measured and the predicated data, with an RMS error of 1.93%.

Except for toluene, the Q_m of the other four hydrocarbons had similar values of about 3400 kJ/kg at a temperature of 750 °C. A chemical heat sink is produced after the thermal decomposition, and it may yield a gaseous product at bulk fluid temperatures above 500 °C [12–15]. In these tests, the gaseous products at steady state were measured at room temperature, and the atmospheric pressure by weight of the liquid products was deducted from the total fuel fed into the system. To reduce or eliminate the deviation caused by the time delay between the inlet and outlet flows from the gas–liquid separator, the liquid product was collected for as long as 3 min and then weighed with an electronic balance. The gasification rates per unit of mass for the five hydrocarbons are shown in Fig. 4. The gasification rate at standard conditions is defined as the ratio of the difference between the standard mass inlet and outlet liquid flow rates to the inlet mass flow rate.

The heat sinks of the endothermic fuels EHF1 and EHF2 were less than those of cyclohexane and n-hexane at temperatures below 600 °C, and there was almost no gaseous product yield. With their higher rates of gasification, the heat sinks of the endothermic fuels and n-hexane rose more quickly than the heat sink of cyclohexane at temperatures of 600–700 °C, as shown in Fig. 3. There was no gaseous product collected for cyclohexane at temperatures of 600 °C or 650 °C, as Fig. 4 shows. However, for n-hexane and EHF2, the gaseous product yields were nearly 30 wt.% and 20 wt.%, respectively, at 650 °C.

Overall, toluene had the best thermal stability of the five hydrocarbons tested. The heat sink of toluene increased linearly with fluid temperature, which indicated that there was almost no chemical heat sink for toluene. The heat sink results for toluene also

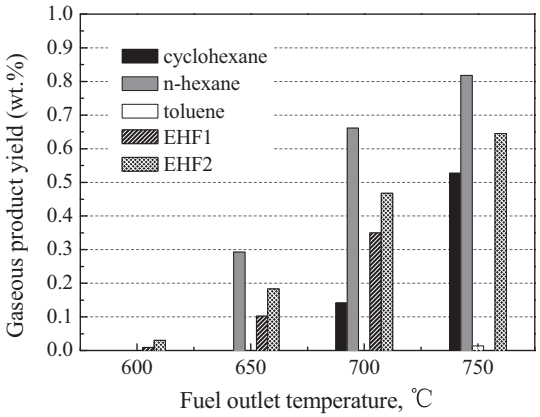

Fig. 4. Gaseous product yields for the five hydrocarbons. Except for the missing data for EHF1 at 750 °C, all of the other vacancies in the data were due to zero yields.

showed that no liquid to gas conversion took place until the temperature reached 750 °C, at which point the gasification rate was only 1.4 wt.%. This result indicated that toluene had good thermal stability, with almost no chemical heat sink observed over the tested range of temperatures up to 750 °C.

A comparison of the volumetric heat sinks of the five hydrocarbons at fluid temperature T_b = 750 °C is shown in Table 4. The volumetric heat sink Q_v represents the heat sink produced by unit of volume by hydrocarbons at 25 °C and atmospheric pressure. Although the mass heat sinks among the five hydrocarbons did not differ greatly, the volumetric heat sinks varied widely due to the hydrocarbons' differing densities. It can be seen that the volumetric heat sinks of cyclohexane and EHF2 were slightly less than that of EHF1, by approximately 4%. However, the Q_v of n-hexane was only 80.38% that of EHF1.

A larger volumetric heat sink indicates that more heat sink can be used per unit volume of hydrocarbon fuel. The test results showed that all of the five hydrocarbons had nearly the same mass heat sink, except for toluene. The ranking order of volumetric heat sink was EHF1 > cyclohexane > EHF2 > n-hexane > toluene.

4.2. Results of deposition propensity

During pyrolysis of hydrocarbons, solid particles with high carbon content are produced and deposited on the inner surface of the test channel, which is called coking [15]. For the non-passivated nickel alloy tubing used in this study, catalytic coke growth on the wall can also occur [2]. Pyrolysis leads to the production of heavy aromatic compounds, such as polycyclic aromatic hydrocarbons (PAH) [27], which can either dissolve in the fluid or condense on the diabatic channel wall to produce coke deposits. When the heavy aromatic compounds dissolve in the fluid, they give the hydrocarbons a deeper color, and these compounds may continue to deposit on the downstream structure surfaces, including the adiabatic channel and the following filter. Coke deposition on the channel's inner wall constricts the flow passage and increases the flow resistance. Therefore, the degree of coke formation can be measured by four methods. These methods are (a) measurement of the pressure drop change during the coking run process, (b) using the HRM for measuring flow resistance in the diabatic and adiabatic channel, (c) evaluating coke deposits in the filter and (d) assessing the color features of the liquid products.

4.2.1. The coking run process for the five hydrocarbons

A large chemical heat sink is produced during the pyrolysis of hydrocarbons, which also causes coke formation on the inner surface of the test channel. Generally, coke formation increases with the increase of fluid temperature [4]. For a diabatic channel exposed to high heat flux, a wall temperature that is much higher than the fuel temperature has a major influence on the level of coke deposition. In our experiment, the coking run was conducted at a fuel outlet temperature of 750 °C for 20 min to accumulate a measurable deposition for evaluation by HRM. However, a sudden increase of pressure or wall temperature caused by a deposition blockage in the channel would burn out the test channel, so that the coking run could break down for hydrocarbons that had a severe propensity for deposition. Therefore, the coking behavior during the coking run process provided a good reference for evaluation.

4.2.1.1. The pure hydrocarbons. All of the three pure hydrocarbons successfully completed the coking run at a fuel outlet temperature of 750 °C for 20 min. This result indicated that the three pure hydrocarbons have fairly good anti-coking qualities. As shown in Table 5, the fluid temperature and pressure were kept steady, with no significant changes before or after fuel pyrolysis. In that situation, the pressure drop in the test channel should not have changed if there was no coke production in the channel. Actually, however, coke was deposited, and the pressure drop of the test channel changed to varying degrees with each of the five hydrocarbons.

The test conditions were maintained at a constant flow rate of 1 g/s for each test fuel, so that the differences in pressure drop were due to the differences in the density of each fuel at standard and reaction conditions. With cyclohexane and n-hexane, the levels of flow resistance in the diabatic channel ΔP_d increased by nearly the same amounts (of 16.3% and 17.2%, respectively). From this result, it could be estimated by equation (2) that about 2% of the channel diameter had been covered by coke deposition. With n-hexane, the adiabatic channel's flow resistance increased by 36%, but with cyclohexane there was almost no change. For toluene, the pressure drop in both channels had no significant change, which was consistent with the previous results showing that almost no cracking reactions happen with toluene at the test conditions.

4.2.1.2. EHF1. The trends of the parameters during pyrolysis for EHF1 are shown in Fig. 5. The fuel temperature ranged from 650 °C to 750 °C with the increase in heating power, and then

Table 4
Comparison of heat sink for the five hydrocarbons at 750 °C.

Hydrocarbons	T_b (°C)	Q_m (kJ/kg)	Percentage Q_m[b] (%)	ρ[a] (g/cm^3)	Q_v (kJ/L)	Percentage Q_v[b] (%)
Cyclohexane	749.8	3465.4	100	0.774	2682.2	96.83
n-Hexane	746.5	3399.3	98.09	0.655	2226.5	80.38
Toluene	749.7	1962.2	56.62	0.862	1691.4	61.06
EHF1	750	3325.3	95.96	0.833	2770.0	100
EHF2	747.6	3391.6	97.87	0.786	2665.8	96.24

[a] Density at 25 °C and atmospheric pressure.
[b] Assuming that the Q_m of cyclohexane is 100% and Q_v of EHF1 is 100%.

Table 5
Comparison of pressure drop before and after coking for the five hydrocarbons.

Parameters		T_b (°C)	P (MPa)	ΔP_d (kPa)	ΔP_a (kPa)
Cyclohexane	Before	748.7	5.04	49.0	39.1
	After	746.4	5.06	57.0	38.8
n-Hexane	Before	747.7	5.04	30.3	26.0
	After	748.6	4.94	35.5	35.4
Toluene	Before	746.9	4.99	18.5	13.9
	After	741.7	4.99	19.1	13.9
EHF1	Before	698.8	5.07	50.2	25.2
	After	694.6	4.91	72.1	36.7
EHF2	Before	748.1	5.09	90.5	27.8
	After	745.8	5.19	97.3	35.3

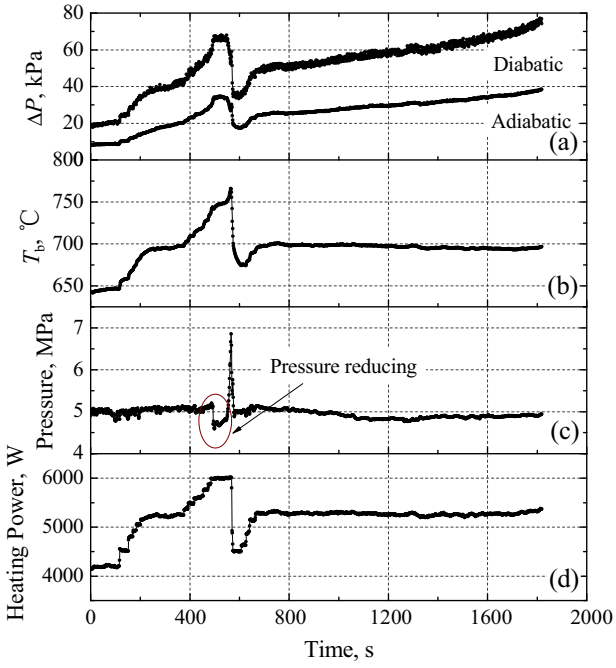

Fig. 5. Profiles of parameters over time during the coking run for EHF1.

the temperature was kept at 700 °C for 20 min. The parameters measured included the diabatic and adiabatic pressure drop, the fuel outlet temperature of the diabatic channel, the pressure, and the heating power.

The pressure rapidly rose from 5 MPa to 7 MPa during pyrolysis at 750 °C, which lasted for no more than 1 min, as seen in Fig. 5. To avoid burnout of the test channel, the heating power was turned down, and the coking run was maintained at a fuel temperature of 700 °C for 20 min. The pressure drops in the diabatic and adiabatic channels were tested before and after the coking run at a fuel outlet temperature of 700 °C. The results are listed in Table 5. The pressure drop increased by 43.6% for the diabatic channel and 45.6% for the adiabatic channel, which indicated that coke deposition during the coking run was significant for both the heated and unheated test channels.

4.2.1.3. EHF2. For EHF2, the coking run persisted at 750 °C for only 10 min, and then the pressure increased uncontrollably in the last 1 min, as shown in Fig. 6. The pressure increased from 5 MPa to 6 MPa in one minute and then suddenly rose to 8.3 MPa in two seconds. Meanwhile, the diabatic pressure rose from 200 to 1660 kPa. To avoid damage to the test channel, the operator turned off the heating power and stopped the coking run at that point.

For EHF2, the flow resistance of the test channel was measured before and after the coking run at a bulk fluid temperature of

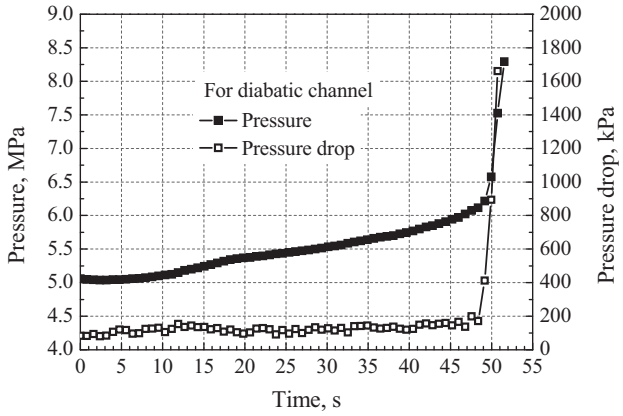

Fig. 6. Parameters over time in the uncontrollable coking process for EHF2.

750 °C. The pressure drop increased by 7.5% for the diabatic channel and 27.0% for the adiabatic channel. It should be noted that the test channel finally became blocked, which caused the pressure drop to suddenly shoot up to 1660 kPa as the fluid temperature reached 789.4 °C. However, the pressure drop is shown in Table 3 as it was measured at 750 °C, to allow the comparison of different hydrocarbons at the same reference temperature. Therefore, the pressure drop in this case cannot be used to judge the final coking characteristic. However, the uncontrollable pressure increase did indicate severe coke deposition.

It should be noted that the trend of the pressure change for EHF2 was different from that for EHF1. The pressure first increased slowly, but could not be controlled by the back pressure regulator at the exit (seen in Fig. 1). This development indicated that the filter gradually accumulated heavy deposits of coke that constricted the fluid flow and gradually increased the pressure. In the case of EHF1, the sudden pressure increase resulted from the pipe being blocked at a downstream location of the pressure tap, which happened due to a big piece of coke peeling off from the coking surface. The pressure curve just before the pressure soared (seen in Fig. 5(c)) provided the evidence that the peeled-off piece of coke was first formed at an upstream location of the pressure tap in the diabatic channel. The breaking off of this piece of coke initially reduced the pressure to some degree. Then the piece of coke flowed downward till it blocked the channel at a downstream location of the pressure tap, causing the pressure to rise suddenly.

4.2.2. Coke deposition measured by HRM

The equivalent coke depositions in the diabatic and adiabatic channels were derived by the corrected HRM and the HRM respectively, and the results are listed in Table 6. To avoid the probably effect of turbulence flow on the results, we calculated the average coke thickness only using the data at laminar flow with low Reynolds number of $Re < 1300$. Although the adiabatic channel was

Table 6
The equivalent thickness of coke layers in the diabatic and adiabatic channels as measured by HRM.

Hydrocarbons	Coke thickness (μm)	
	Diabatic	Adiabatic
Cyclohexane	57	60
n-Hexane	9	112
Toluene	61.5	0
EHF1	108	68
EHF2	156	90

thermally insulated, the bulk fuel temperature decreased by no more than 30 °C across the channel over the full fuel temperature range. The coke thickness values of the adiabatic channel for n-hexane, EHF1 and EHF2 were quite large, which was consistent with the results showing the pressure drop changes before and after coking runs at a fluid temperature of 750 °C. For EHF1, the diabatic channel had the second largest coke layer, as can also be seen in the pressure drop data shown in Table 5. The diabatic channel in EHF2 had the largest coke layer, which was also accordant with the most severe coking run characteristics.

It can be seen that the pressure drop changes in Table 5 to some degree deviated from the results of equivalent coking deposition shown in Table 6, especially for the diabatic channel with n-hexane and toluene. But it is rational that the toluene has no coke formation in the adiabatic channel. Because the toluene almost had no thermal cracking, which was indicated by the heat sink results in Fig. 3 with no chemical heat sink and the gaseous products in Fig. 4 with almost no gaseous produced. It should be noted that the results shown in Table 5 were obtained with hydrocarbon fluids flowing through the test channel at high temperature and high pressure. The results shown in Table 6, however, were derived from the pressure drop data at ambient temperatures and atmospheric pressure. The results in Table 6 probably have some additional deviations during the cooling process for the test channel after the end of coking run, such as pieces of coke being washed away by the cool hydrocarbon flow, or new coke being produced on the channel wall as the cool hydrocarbon reacted with the high temperature channel surface.

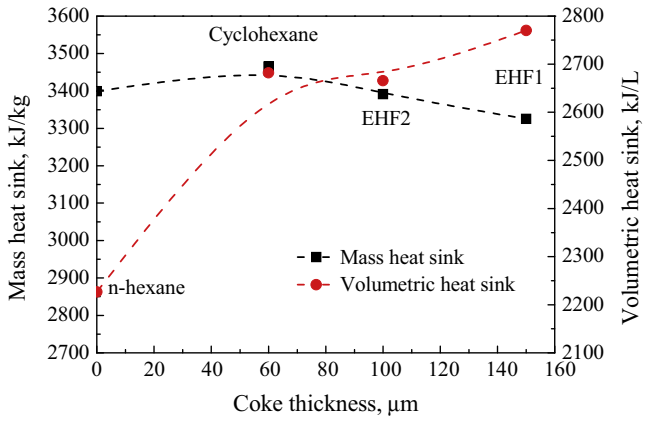

Fig. 7. Comparison of heat sinks with coke deposits in the adiabatic channel for different fuels.

Comparisons of the mass heat sink and the volumetric heat sink with coke deposits in the adiabatic channel were conducted for different fuels, as shown in Fig. 7. The mass heat sink had a slight decrease at higher coke rates, but the volumetric heat sink increased significantly with thicker coke deposition. Cyclohexane had the biggest mass heat sink and a relatively larger volumetric heat sink, with less coking propensity. The endothermic fuels EHF1 and EHF2 had large volumetric heat sinks, but also caused huge productions of coke.

4.2.3. Color features of liquid products

Heavy aromatic compounds produced and dissolved in the liquid products changed the color features of the liquids. The total aromatic contents in the liquid products and the deposition rates were found to have very strong correlations with the cracking rate (liquid to gas conversion) [9]. Fig. 8 shows the color features of the liquid products after reacting at various fluid temperatures ranging from 100 °C to 750 °C. All of the hydrocarbon liquid samples were

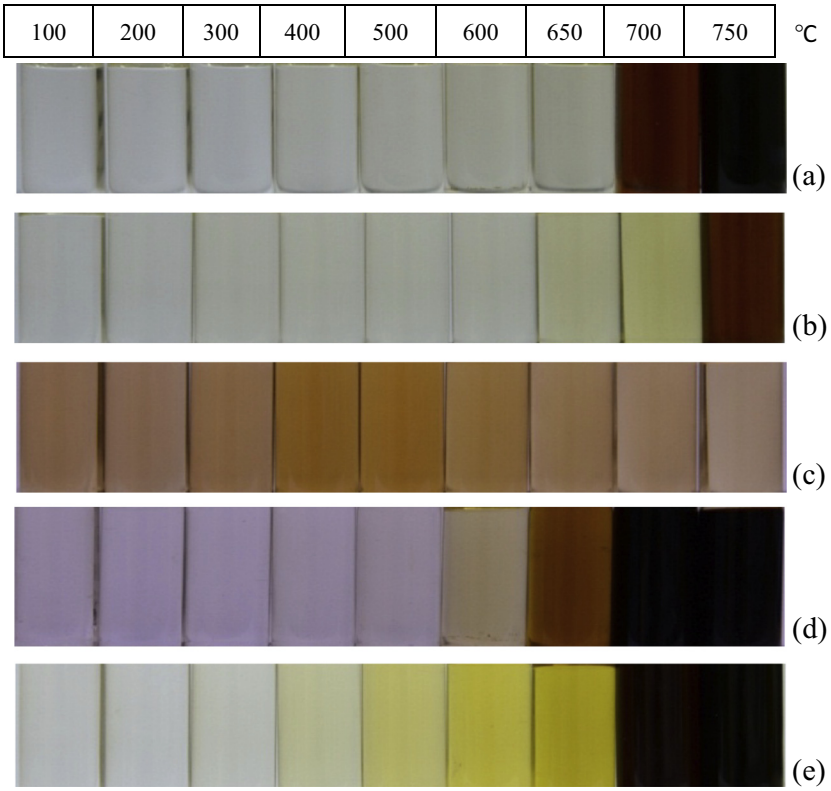

Fig. 8. Color features of liquid products at various fuel temperatures for the five hydrocarbons.

colorless and transparent at room temperature. At temperatures below 400 °C, the color of the liquid products showed no change, as almost no thermal decomposition was taking place. The color of the liquids became deeper with increases of temperature over 400 °C. At 750 °C, EHF1 and EHF2 and cyclohexane had the darkest colors, being nearly black, which indicated the massive formation of carbonaceous compounds in the liquid products. For n-hexane and toluene, lighter fuel colors indicated that lesser amounts of heavy aromatic compounds were present.

The color features were not analyzed by colorimeter (spectrophotometry) in this study, as this was not thought to be necessary. Actually, however, a few dissolved carbon particles could lead to darker color in the fuel, and therefore a quantitative analysis of the color feature could not provide definite results such as measures for the amounts of coke in the bulk fuel products. For the purposes of this study, it was enough to discern whether the fuel product became black at the relevant fuel temperature. It should be explained that in theory, the color of toluene should not have changed, as almost no cracking happened. Actually however, toluene did grow darker as the temperature changed between 100 °C to 750 °C. This fuel was darkest at between 400 °C and 500 °C, which could have resulted from causes other than the thermal decomposition, such as oxidation and impurities.

4.2.4. Deposition in the filter

In this set of experiments, a 0.2 mm copper sintering filter was placed after the adiabatic channel. Between the adiabatic channel and the filter there was a set of connection tubes that had no heat protection. These tubes allowed the reacted fuel flowing through them to be cooled to about 600 °C, as compared to the 750 °C temperature at the fuel outlet of the diabatic channel. The coke particles (or PAH) that had dissolved in the bulk fuel condensed out and were deposited in the filter as the temperature cooled, due to a decrease in the solubility of the high molecular weight species. In addition, the space in the filter was larger than the test channel, so the retention time for the bulk fuel was much longer in the filter than in the test channel, which led to more coke production. At every coking run, a new filter cartridge (shown in Fig. 9(e)) was placed in the filter. It can be seen in Fig. 9 that the surface of the filter used with toluene acquired a metallic color. With n-hexane, part of the surface was metallic yellow, but with cyclohexane all of the surface was covered with coke and became dark. This set of results indicated that the comparative levels of coke deposition for the pure hydrocarbons were cyclohexane > n-hexane > toluene. EHF1 and EHF2 had the highest levels of coke deposition. With EHF2 it could be clearly seen that the filter's surface was surrounded by a thick coke layer, and with EHF1 the filter was covered by a thin coke layer. The massive coke production in the filter with EHF2 also verified the uncontrollable pressure rise shown in Fig. 6.

The amounts of coke deposited on the filter elements with each hydrocarbon can be ranked as EHF2 > EHF1 > cyclohexane > n-hexane > toluene. In addition, the results for EHF1 were obtained at a fuel outlet temperature of 700 °C. The results of the coke accumulated in the filter entirely agree with the fuel color features, showing that heavy coke deposition was accompanied with a dark color of the liquid products, which could indicate that the coke deposition in the filter was condensed from the liquid products.

5. Discussions

5.1. The effect of wall temperature on coke deposition

The rates of coke deposition from endothermic fuel during pyrolysis are mainly affected by the factors of fuel composition [9], fuel temperature [11,12], wall temperature [11], system pressure [10,11] and residence time [12]. The effects of fuel temperature and wall temperature are discussed below.

The profiles of wall temperature along the diabatic channel for the five hydrocarbons (at a fluid outlet temperature of 750 °C) are shown in Fig. 10(a). In this figure the sketchy profile of bulk fluid temperatures (for the other four hydrocarbons except toluene) were estimated according to the measured heat sinks in Fig. 3. The hydrocarbons entered the test channel at about 25 °C, and the bulk fuel temperatures increased to 750 °C at the 15th TC point near the outlet. At the 9th TC point (8/14 of the length) the bulk fuel temperatures were estimated as 600 °C when the heat sink values were about 2000 KJ/kg, 8/14 of the total heat sinks of about 3500KJ/kg. The fuel temperatures between 25 °C and 600 °C and between 600 °C and 750 °C were linearly connected.

Except for toluene, the wall temperatures at the same location of the test channel for the other four hydrocarbons had small differences at fluid temperatures above 400 °C. The coking rates (coke amounts averaged over the channel inner surface) as a function of the wall temperatures for the diabatic channel are shown in Fig. 10(b). After the reaction, the diabatic channel was carefully cut into 50 mm sections by wire electrical discharge machining (WEDM). After drying in an oven at 100 °C, the short sections were weighed by a Sartorius electronic balance with a precision of 0.01 mg. The coke deposition on each section could then be measured by the weight of the coked tube minus the mass of the blank tube, which was calculated from the volume and material density.

Although the wall temperatures were similar for all of the tested fuels, the coking rates of the endothermic fuels were still much greater than those of the pure hydrocarbons, which indicated that fuel composition had a significant effect. Also, it was noted that the coking rates considerably increased at wall temperatures over 700 °C for both endothermic fuels and for pure hydrocarbons. Undoubtedly, these increases in coking rates resulted from high wall temperatures rather than fluid temperatures, because the wall temperatures approached 700 °C as the bulk fuel temperatures remained at 500 °C. At 500 °C, the fuels had almost no change in color, and almost no thermal decomposition occurred. These results indicated that coking behavior was most probably a

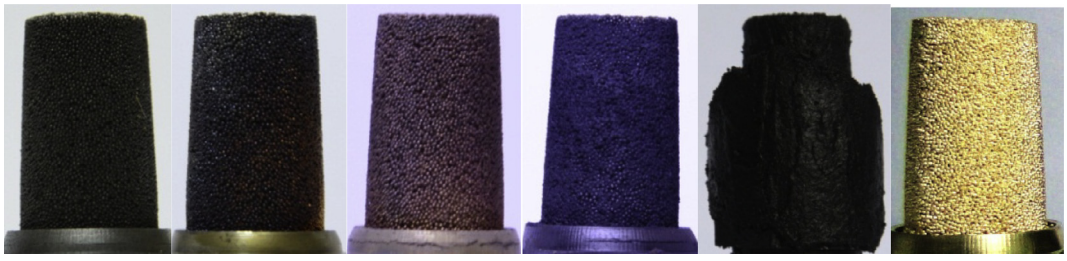

(a) Cyclohexane (b) n-hexane (c) Toluene (d) EHF1 (e) EHF2 (e) Blank

Fig. 9. Coke deposits on the filter elements after coking runs for different hydrocarbons.

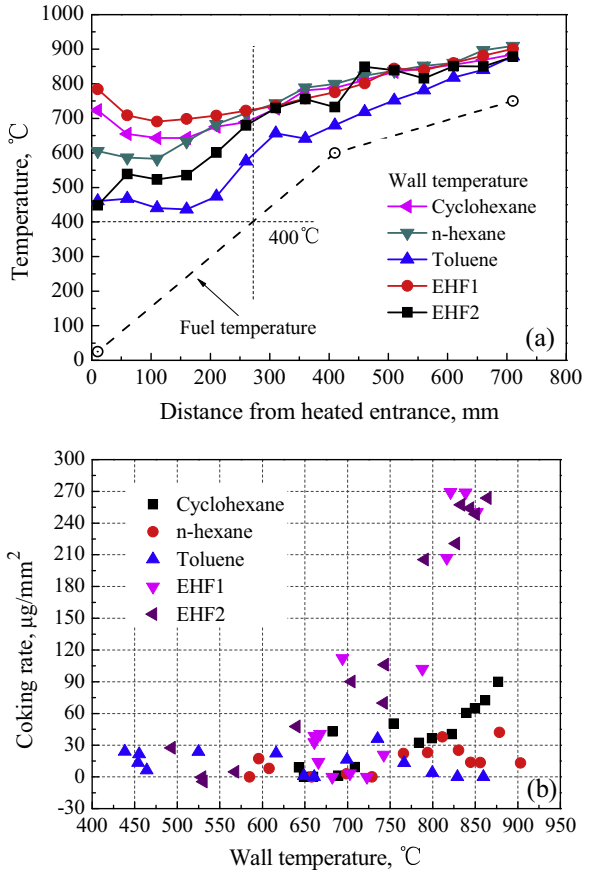

Fig. 10. Coking rate as a function of wall temperature for the diabatic channel.

process occurring in the thermal boundary layer of the fluid near the wall.

5.2. Effect of deposition on the wall temperature

Coke deposition on the channel surface creates a thermal layer that reduces the heat transfer efficiency between the wall and the fluid. Therefore, coking should increase the wall temperature. However, it was found that the wall temperature did not necessarily increase when considerable layers of coke were deposited on the inner surface of the test channel.

The profiles of wall temperature over time at designated TC points during the coking run at steady state are shown in Fig. 11.

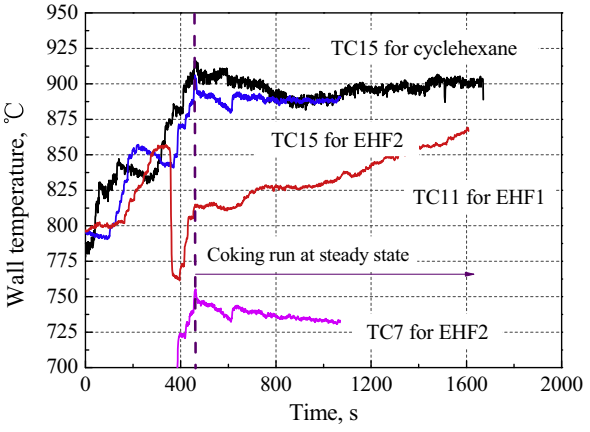

Fig. 11. Effects of coking on the wall temperature for different hydrocarbons.

These measurements showed that the same coking rate of 90 μg/mm^2 occurred at TC7 with EHF2, TC11 with EHF1 and TC15 with cyclohexane, but the wall temperatures behaved differently with each of these hydrocarbons. At TC7 with EHF2, the wall temperature gradually decreased during the whole coking run process. At TC11 with EHF1, the wall temperature decreased and then increased. At TC15 with cyclohexane, the wall temperature gradually increased throughout the process. At TC15 for EHF2, the wall temperature was almost unchanged during the coking run, even though the coking rate approached 270 μg/mm^2 at the end of coking run.

These results indicated that the changes in wall temperature could be influenced by other factors besides the thickness of the coke layer. The two parameters of wall temperatures and the thickness of the coke layers did not have a strong functional relationship, which indicated a complicated problem that will be valuable to investigate in the future.

6. Conclusions

In this study, a set of approaches was proposed to evaluate the heat sink capability and deposition propensity of supercritical endothermic fuels in a minichannel at temperatures up to 750 °C. Experimental tests were conducted for three pure hydrocarbons (cyclohexane, n-hexane and toluene), one petroleum-derived kerosene and one synthetic fuel modeled as endothermic fuels. The conclusions of these tests were as follows:

(a) The approaches proposed for evaluating the heat sink and coking characteristics of endothermic fuel were proved to be feasible and convenient. The parameter changes during the coking run process, the color features of the liquid products and the coke depositions in the filter could be used to qualitatively measure the coking characteristics of each fuel. The HRM (hydraulic resistance method) could be used to semi-quantitatively measure the amount of coke production. This experimental evaluation system for selecting fuel candidates can make fuel research and development more efficient.

(b) The heat sink and coking characteristics are two contrary qualities in endothermic fuels. All of the five tested hydrocarbons had a similar heat sink of about 3.4 MJ/kg at 750 °C. However, the volumetric heat sinks of these hydrocarbons were different due to their varying densities (at 25 °C). The endothermic fuels had the largest volumetric heat sink, but the worst anti-coking capacity, which was converse to the qualities of toluene and n-hexane. In balance, the cyclohexane had a relatively bigger heat sink and less coking propensity.

(c) The petroleum-derived kerosenes were more prone to produce coke than the pure hydrocarbons. The levels of coke formation were influenced by a set of complicated factors, including fuel composition, fuel temperature and wall temperature. However, the effects of coke layers on the wall temperature were uncertain. Clearly, the thickness of the coke layers and the thermal resistance they provided were not the only factors affecting wall temperatures, and these results require further investigation.

Acknowledgments

This study was sponsored by the National Natural Science Foundation of China (Grant No. 21306147), the China Postdoctoral Science Foundation (Grant No. 2013M532044) and the Fundamen-

tal Research Funds for the Central Universities. Their financial support is gratefully acknowledged.

References

[1] Lander H, Nixon AC. Endothermic fuels for hypersonic vehicles. J Aircr 1971;8:200–7.
[2] DeWitt MJ, Edwards T, Shafer L, et al. Effect of aviation fuel type on pyrolytic reactivity and deposition propensity under supercritical conditions. Ind Eng Chem Res 2011;50:10434–51.
[3] Mikhaylov AM. The use of supercritical endothermic fuel. J Phys Conf Ser 2013;461:012–35.
[4] Edwards T. Liquid fuels and propellants for aerospace propulsion: 1903–2003. J Propul Power 2003;19:1089–107. AIAA 2003-6946.
[5] Huang H, Sobel DR, Spadaccini LJ. Endothermic heat-sink of hydrocarbon fuels for scramjet cooling. In: 38th AIAA/ASME/SAE/ASEE Joint Propulsion Conference & Exhibit 2002; AIAA 2002-3871.
[6] Zhou W, Jia Z, Qin J, et al. Experimental study on effect of pressure on heat sink of n-decane. Chem Eng J 2014;243:127–36.
[7] Bates RW, Edwards T. Heat transfer and deposition behavior of hydrocarbon rocket fuels. In: 41st Aerospace Sciences Meeting and Exhibit 2003; AIAA 2003-123.
[8] Van Noord JL, Stiegemeier BR. Thermal stability and heat transfer investigation for hydrocarbon boost engines. NASA Report 2010; NASA/TM, 2010-216917.
[9] Edwards, T. Fuel composition influence on deposition in endothermic fuels. In: 14th AIAA/AHI Space Planes and Hypersonic Systems and Technologies Conference 2006; AIAA 2006-7973.
[10] Ledesma EB, Wornat MJ, Felton PG, et al. The effects of pressure on the yields of polycyclic aromatic hydrocarbons produced during the supercritical pyrolysis of toluene. Proc Combust Inst 2005;30:1371–9.
[11] Corporan E, Minus DK. Studies of decalin as a suppressor of pyrolytic deposits in JP-8+100. In: 35th AIAA/ASME/SAE/ASEE Joint Propulsion Conference and Exhibit 1999; AIAA 1999-2213.
[12] Herbinet O, Marquaire PM, Leclerc FB, et al. Thermal decomposition of n-dodecane experiments and kinetic modeling. J Anal Appl Pyrolysis 2007;78:419–29.
[13] Edwards T, Anderson SD. Results of high temperature JP-7 cracking assessment. In: 31st Aerospace Sciences Meeting & Exhibit 1993; AIAA 1993-0806.
[14] Bouchez M, Daniau E, Visez N, et al. Hydrocarbon heterogeneous pyrolysis experiments and modeling for scramjet thermal management. In: 15 AIAA International Space Planes and Hypersonic Systems and Technologies Conference 2008; AIAA 2008-2623.
[15] Fau G, Gascoin N, Steelant J. Hydrocarbon pyrolysis with a methane focus – a review on the catalytic effect and the coke production. J Anal Appl Pyrolysis 2014;108:1–11.
[16] Linne DL, Meyer ML, Edwards T. Evaluation of heat transfer and thermal stability of supercritical JP-7 fuel. AIAA 1997-3041.
[17] Gascoin N, Abraham G, Gillard P. Thermal and hydraulic effects of coke deposit in hydrocarbon pyrolysis process. J Thermophys Heat Transfer 2012;26:57–65.
[18] Deng HW, Zhang CB, Xu GQ, et al. Density measurements of endothermic hydrocarbon fuel at sub- and supercritical conditions. J Chem Eng Data 2011;56:2980–6.
[19] Deng HW, Zhang CB, Xu GQ, et al. Viscosity measurements of endothermic hydrocarbon fuel from (298 to 788) K under supercritical pressure conditions. J Chem Eng Data 2012;57:358–65.
[20] Edwards T. "Kerosene" fuels for aerospace propulsion – composition and properties. In: 38th AIAA/ASME/SAE/ASEE Joint Propulsion Conference & Exhibit 2002; AIAA 2002-3874.
[21] Shafer L, Striebich R, Gomach R, et al. Chemical class composition of commercial jet fuels and other specialty kerosene fuels. In: 14th AIAA/AHI Space Planes and Hypersonic Systems and Technologies Conference 2006; AIAA 2006-7972.
[22] Brown SP, Frederick RA. Laboratory-scale thermal stability experiments on RP-1 and RP-2. J Propul Power 2008;24:206–12.
[23] Liu ZH, Bi QC, Guo Y, et al. Hydraulic and thermal effects of coke deposition during pyrolysis of hydrocarbon fuel in a mini-channel. Energy Fuels 2012;26:3672–9.
[24] Liu ZH, Bi QC, Guo Y, et al. Heat transfer characteristics during subcooled flow boiling of a kerosene kind hydrocarbon fuel in a 1 mm diameter channel. Int J Heat Mass Transfer 2012;55:4987–95.
[25] Liu ZH, Bi QC, Guo Y, et al. Convective heat transfer and pressure drop characteristics of near-critical-pressure hydrocarbon fuel in a mini-channel. Appl Therm Eng 2013;51:1047–54.
[26] Liu ZH, Bi QC, Ma XS, et al. Thermal induced static instability of hydrocarbon fuel in the regeneratively cooled structures of hypersonic vehicles. In: 18th AIAA/3AF International Space and Hypersonic Systems and Technologies Conference, 2012; AIAA 2012-5859.
[27] Edwards T. Cracking and deposition behavior of supercritical hydrocarbon aviation fuels. Combust Sci Technol 2006;178:307–34.